



Published in final edited form as:

Biochem Pharmacol. 2008 January 15; 75(2): 570–579.

Characterization of mouse flavin-containing monooxygenase transcript levels in lung and liver, and activity of expressed isoforms

Lisbeth K. Siddens, Marilyn C. Henderson, Jonathan E. VanDyke, David E. Williams, and Sharon K. Krueger

Department of Environmental and Molecular Toxicology and The Linus Pauling Institute, Oregon State University, Corvallis, OR 97331

Abstract

The significance of active vs. inactive flavin-containing monooxygenase 2 (FMO2) for human drug and xenobiotic metabolism and sensitivity is unknown, but the underlying ethnic polymorphism is well documented. We used quantitative real-time PCR to measure message levels of *Fmo1*, *Fmo2*, *Fmo3* and *Fmo5* in lung and liver from eight strains of eight week old female mice to determine if a strain could be identified that predominately expressed *Fmo2* in lung, recapitulating the human *FMO* expression profile and being the ideal strain for *Fmo2* knockout studies. We also characterized enzyme activity of baculovirus expressed mouse *Fmo1*, *Fmo2* and *Fmo3* to identify a substrate or incubation conditions capable of discriminating *Fmo2* from *Fmo* mixtures. *Fmo* transcript expression patterns were similar for all strains. In lung, 59% of total *FMO* message was *Fmo2*, but *Fmo1* levels were also high, averaging 34%, whereas *Fmo3* and *Fmo5* levels were 2 and 5%, respectively. In liver, *Fmo1*, *Fmo2*, *Fmo3* and *Fmo5* contributed 16, 1, 7 and 76% respectively, of detected message. Peak activity varied by isoform and was pH- and substrate-dependent. *Fmo3* oxidation of methyl *p*-tolyl sulfide was negligible at pH 9.5, but *Fmo3* oxidation of methimazole was comparable to *Fmo1* and *Fmo2*. Heating microsomes at 50 °C for 10 min eliminated most *Fmo1* and *Fmo3* activity, while 94% of *Fmo2* activity remained. Measurement of activity in heated and unheated lung and liver microsomes verified relative transcript abundance. Our results show that dual *Fmo1/2* knockouts will be required to model the human lung *FMO* profile.

Keywords

quantitative real-time PCR; in vitro expression; flavin-containing monooxygenase; mouse; pulmonary expression; hepatic expression

1. Introduction

Mammalian flavin-containing monooxygenases (FMO, EC 1.14.13.8) are microsomal phase I enzymes that incorporate an atom of molecular oxygen into a wide range of nitrogen- and sulfur-containing drugs and xenobiotics (reviewed in Krueger and Williams 2005 [1]).

Although oxygenation usually represents a detoxication reaction, some FMO-oxygenated

Corresponding author: Dr. Sharon K. Krueger, Linus Pauling Institute, Oregon State University, 571 Weniger Hall, Corvallis, OR 97331-6512. Tel. (541)737-9322; Fax (541)737-5077; E-mail sharon.krueger@oregonstate.edu.

Publisher's Disclaimer: This is a PDF file of an unedited manuscript that has been accepted for publication. As a service to our customers we are providing this early version of the manuscript. The manuscript will undergo copyediting, typesetting, and review of the resulting proof before it is published in its final citable form. Please note that during the production process errors may be discovered which could affect the content, and all legal disclaimers that apply to the journal pertain.

sulfur substrates, such as thioureas, produce reactive sulfenic or sulfinic acids as major metabolites. Sulfenic acid metabolites can react with GSH inducing oxidative stress through a futile redox cycle [2-5].

Humans have five *FMO* genes (*FMO1-5*) and six pseudogenes (*FMO6P-11P*) [6-8], while mice have nine *FMO* genes (*Fmo1-6, 9, 12* and *13*) [7]. *FMO1*, *FMO2* and *FMO3* are the major mammalian drug and xenobiotic metabolizing isoforms from all species studied to date and are expressed in a tissue-, species-, sex-, and developmental-specific manner. In human and most other species including rabbit, monkey and guinea pig, *FMO2* is expressed at high levels in lung and is the predominant drug metabolizing isoform in this organ [9-14]. *FMO2* is co-expressed with other isoforms in kidney, intestine and nasal mucosa but is not the predominant *FMO* in these tissues.

A genetic polymorphism (g.23,238C>T; dbSNP#rs6661174) in human *FMO2* converts a glutamine to a stop codon, p.Q472X [15]. Protein encoded by this allele (*FMO2*2*) does not bind FAD and is inactive [15,16]. This polymorphism is present in all Caucasians and Asians genotyped to date [15,17]. The *FMO2*1* allele encoding full-length active protein is estimated to occur in 13-26% of individuals of African descent [17,18] and 2-7% of Hispanic origin [19,20]. Other polymorphisms of *FMO2* have been documented [15,17,18], but are expected to be of minor impact as most are found exclusively or primarily as mutations secondary to the *FMO2*2* allele [15,17,21].

Expressed human *FMO2.1* efficiently catalyzes the oxidation of thioethers [22] and thioureas [5]. Ethnically- and racially-dependent differences may exist for metabolism upon exposure to these or other classes of compounds in the form of drugs (e.g. thioureas) and insecticides (e.g. thioethers), thus we are working to develop an animal model to test the relevance of these alterations. The *FMO2* allele from laboratory rat strains (*Rattus norvegicus*) encodes truncated, inactive protein [23] but in a wild population from this species there is segregation for the wildtype and mutant *FMO2* alleles [24]. Wild rats are not ideal to work with given that they were found to produce enzymatically active *FMO1* in addition to *FMO2* (in rats with at least one wildtype allele) [24], and any animals entering animal housing would need to undergo extensive cleanup to free them of infectious organisms that could threaten the health of other laboratory rodents.

The laboratory mouse (*Mus musculus*) represents a potentially viable alternative model. Because all tested mice have alleles encoding intact, active *Fmo2*, a knockout would be required to recapitulate the common human allelic variant. Studies from mice have conflicting results regarding the presence and abundance of *Fmo2* in mouse lung. A 1992 study [25] demonstrated the presence of *Fmo1* and *Fmo2* transcript and protein in lung. More recently, a study of *FMO* gene expression in mice identified *Fmo1* not *Fmo2* as the major lung isoform [26]. We conducted this study to determine whether we could identify a mouse strain that primarily produced *Fmo2* in the lung, as *Fmo2* substrates would likely also be substrates for *Fmo1*, and would thus confound studies of *Fmo2*. In addition, we performed enzyme assays with methimazole (MMI) and methyl *p*-tolyl sulfide (MTS) as substrate for expressed *Fmo1*, *Fmo2* and *Fmo3* in search of conditions that could distinguish contributions by individual *FMO* isoforms.

2. Materials and Methods

2.1 Experimental animals

Four eight- week old, female mice of six different inbred strains and one hybrid strain were purchased from The Jackson Laboratory (Bar Harbor, ME). One additional outbred strain was purchased from Harlan (Indianapolis, IN) (Table 1). Tissues for RNA extraction were

recovered from mice upon their arrival at the Laboratory Animal Resource Center at Oregon State University. All procedures were conducted according to National Institutes of Health guidelines and were approved by the Oregon State University Animal Care and Use Committee.

Frozen lungs and livers from 8 to 10 week old female Swiss Webster mice were purchased (Pel-Freez, Rogers, AR) for the preparation of microsomes. Lungs and livers were not necessarily from the same mice. Upon receipt, tissue was stored at -80 °C until microsomes were prepared by differential centrifugation [27] from two pools each of 15 lung pairs and five livers. Protein concentrations were subsequently determined [28].

2.2 Tissue harvest and RNA extraction

Lungs and livers were harvested from mice euthanized with an overdose of CO₂. Tissues were immediately placed in Trizol® reagent (Invitrogen, Carlsbad, CA), snap frozen in liquid nitrogen and stored at -80 °C until total RNA was extracted per manufacturer's recommendation. RNA was further purified with RNeasy (Qiagen, Valencia, CA). RNA quality was measured on an Agilent 2100 Bioanalyzer (Santa Clara, CA) and quantitated with a NanoDrop ND-1000 UV-Vis spectrophotometer (Wilmington, DE).

2.3 DNA synthesis and real-time PCR

For each sample 2.0 µg RNA was treated with amplification grade DNase I (Invitrogen) and then reverse transcribed following Invitrogen's recommendations using Superscript III and random hexamers (Invitrogen), as not all FMOs have an apparent poly-A tail. dNTPs were from Fermentas Inc. (Hanover, MD). Reactions were run on a PTC-100 ThermalCycler (MJ Research Inc., Waltham, MA), 25 °C for 5 min, 42 °C for 1 h, and 70 °C 15 min. cDNA reaction volumes were brought to 50 µl with nuclease free water and stored at 4 °C until quantitative PCR was completed for all of the genes of interest.

Gene-specific primer pairs (Table 2) were synthesized (Invitrogen) and used to produce DNA amplicons for real-time PCR calibration curves, and for amplification reactions with test samples. In addition to mouse *Fmo1-3*, and *Fmo5*, four housekeeping genes including cytoplasmic β-actin (*Actb*), hypoxanthine guanine phosphoribosyl transferase 1 (*Hprt1*), large ribosomal protein 13a (*Rpl13a*), and TATA box binding protein (*Tbp*) were quantitated from lungs and livers from all mice.

Gene-specific standards were constructed to quantitate each gene target. Lung and liver cDNA from eight mice was pooled and PCR products generated using the conditions for real-time PCR reactions described below, except that melt curve analysis was not performed. PCR products were electrophoresed on agarose gels then purified with a Zymoclean™ Gel DNA Recovery kit (Zymo Research Corp., Orange, CA), quantitated with Quant-iT™ Picogreen® (Molecular Probes, Eugene, OR) and diluted to cover a 10⁶-fold range for calibration curves, using reactions containing 0.0001 pg to 100 pg gel-purified DNA.

Real-time PCR reactions contained 1.0 µl cDNA template (or appropriately diluted DNA standard), 0.4 µM forward primer, 0.4 µM reverse primer, 10 µl 2X DyNAmo™ SYBR® green master mix (New England Biolabs, Ipswich, MA), and water to 20 µl. PCR was performed in an MJ Research (BioRad Research, Hercules, CA) Opticon 2 thermal cycler using Opticon Monitor version 3.1 software (BioRad Research). Reactions were initially denatured at 95 °C for 10 min followed by 35 cycles of 10 s denaturing at 94 °C, 20 s annealing (see Table 2 for specific temperatures), 18 s extension at 72 °C, an extension step for 7 min at 72 °C, melt curve at 50-93 °C at 0.2 °C intervals, and a final extension for 10 min at 72 °C. In order to determine whether primer pairs amplified a single product of the correct size we used both Opticon Monitor software's melt curve analysis and gel electrophoresis. Products were run on 6% TBE

gels (Invitrogen) and visualized by ethidium bromide staining. Results from each of the four housekeeping genes were considered separately and as the geometric mean of all four, to determine the most appropriate gene for normalizing real-time reactions for *Fmo1-3*, and *Fmo5*. Normalized data were expressed as a ratio of the calculated values (copies *Fmo* isoform/ μg total RNA : copies *Hprt1*/ μg total RNA) for each sample.

Statistical analysis was done using InStat software (GraphPad Inc., San Diego, CA). Bartlett's test was used to determine whether groups exhibited similar variance. Those groups with significant difference in variance were ln transformed ($Y=\ln Y$) before analyzing. Strain differences for each FMO isoform and levels of expression within each strain were compared with one-way ANOVA followed by a Tukey's multiple comparisons test when significant differences ($p < 0.05$) of means occurred.

2.4 cDNA synthesis, cloning and protein expression

First strand cDNA synthesis was performed on RNA (2.0 μg) isolated from a female F1 Hyb mouse liver (*Fmo1* and *Fmo3*) and lung (*Fmo2*) using SuperScript III (Invitrogen) according to Invitrogen's recommendations. The final reaction volume was 40 μl . *Fmo*-specific reverse primers (Table 3) were used in the reaction at a final concentration of 0.1 μM (2 pmol/ μg RNA). First strand PCR conditions were the same as described above for cDNA used in quantitative PCR. First strand synthesis product was diluted to 100 μl with water; 4 μl was subsequently used as template in 20 μl PCR reactions with 1 unit Expand High Fidelity polymerase (Roche, Indianapolis, IN) and *Fmo*-specific forward and reverse primers (Table 3) at 0.2 μM , each. Robocycler (Stratagene, La Jolla, CA) conditions were: 4 cycles of 45 s at 94 $^{\circ}\text{C}$, 45 s at 56 $^{\circ}\text{C}$, 120 s at 72 $^{\circ}\text{C}$; 30 cycles of 30 s at 94 $^{\circ}\text{C}$, 30 s at 56 $^{\circ}\text{C}$, 90 s at 72 $^{\circ}\text{C}$; the extension time was extended by 10 min in the final cycle.

Full-length cDNA products were cloned into pENTR/SD/D-TOPO (Invitrogen) and expressed in Sf9 cells. Plasmid DNA was isolated (Qiagen) and cDNA sequenced (Center for Genome Research and Biocomputing, Oregon State University, Corvallis, OR), to confirm that translated sequences matched the corresponding NCBI reference sequences [NP_034361](#), [NP_061369](#) and [NP_032056](#) for *Fmo1*, *Fmo2* and *Fmo3*, respectively. Vector DNA from each of the clones was recombined with BaculoDirect linear DNA (Invitrogen) to yield recombinant baculovirus DNA for transfection of Sf9 cells to generate primary virus. Recombinant protein was produced for each clone as described previously [21,22] with the addition of FAD to the media (10 $\mu\text{g}/\text{ml}$) of batches that microsomes were isolated from. Microsomes were isolated [16] from cells harvested 96 h post-infection and were resuspended in storage buffer (10 mM potassium phosphate pH 7.4, 20% glycerol, 1 mM EDTA, 100 mM phenylmethylsulfonyl fluoride). Protein concentration was determined by the Bradford method [28]. FMO content was calculated from HPLC determination of FAD content [22].

2.5 Enzyme assays

Enzyme activity was estimated for expressed mouse *Fmo1*, *Fmo2* and *Fmo3* by following MMI-dependent oxidation of TNB [29] as detailed previously [16], except that MMI was from Lancaster Synthesis (Ward Hill, MA), or by following MTS oxidation, as detailed below. The limit of detection for the MMI assay in our laboratory was 0.035 nmol TNB oxidized min^{-1} (corresponding to 0.1, 0.5 and 0.3 pmol of *Fmo1*, *Fmo2* and *Fmo3*, respectively, at pH 8.5). Benchmarking assays were performed daily to confirm that assay run variability did not exceed 10%. Study parameters included pH profiles (pH 7.5 to 9.5) performed with MTS (200 μM) and MMI (2 mM) as substrate; sodium cholate addition (0, 1 and 1.5%) with MMI (2 mM) at pH 8.5; and activity retention following heat treatment (all proteins were diluted to 3 mg/ml in storage buffer for the 10 min pre-incubation at 50 $^{\circ}\text{C}$) at pH 8.5 using MMI (2 mM), or pH 9.5 using MTS (200 μM). Kinetic constants for MTS oxidation (2 to 20 μM substrate) were

calculated for Fmo1 and Fmo2 at pH 9.5, from two independently expressed replicates of each isoform using Lineweaver-Burk and Eadie-Hofstee plots. A two-tailed unpaired t-test (InStat software, GraphPad Inc.) was used to test for significance of kinetic estimates; data were ln transformed when variances were not equal.

Oxidation of MTS was analyzed by the method of Rettie, *et al.* [30] with some modifications. MTS and methyl *p*-tolyl sulfoxide (MTSO, racemic mixture and individual enantiomers) were from Sigma-Aldrich (St. Louis, MO). Standard microsomal incubations contained 100 µg of expressed protein in a total reaction volume of 250 µl (0.1 M Tricine pH 9.5, 1 mM EDTA, 1 mM NADPH). After 3 min preincubation on ice, reactions were initiated by the addition of MTS and transferred to a Dubnoff shaking incubator at 37 °C. Reactions were stopped after 5 min (2.5 min for kinetics) by addition of 75 µl acetonitrile on ice. After centrifugation at 10,000 × *g* for 30 min at 4 °C, supernatants were analyzed by HPLC with a Waters 2695 system (Waters Corp., Milford, MA) equipped with a photodiode array detector. MTSO was separated from MTS on a Waters Novapak C₁₈ (150 × 3.9 mm) column at 40 °C, a flow rate of 0.8 ml/min and detection at 237 nm. Mobile phase was 30% acetonitrile for 4 min; to 80% acetonitrile in 2 min; returned to 30% acetonitrile at 8 min, in 2 min. The retention times of racemic MTSO and MTS were 2.7 and 8.7 min, respectively. Standard curves ($r^2 = 0.9965$) of racemic MTSO (0.5 to 5 nmol) were run each day of analysis and MTSO values calculated by linear regression with a detection limit of 50 pmols.

For determination of the (*S*)-(-)- and (*R*)-(+)-MTSO enantiomers, incubations were stopped by placing them on ice and extracting twice with 1.0 ml ethyl acetate. The combined extracts were dried under vacuum with a Savant speed-vac (Thermo Scientific, Waltham, MA) and dissolved in 50 µl hexane:isopropyl alcohol (90:10) for analysis by chiral HPLC. The MTSO enantiomers were separated on a Phenomenex (Torrance, CA) Chirex (R)-PGYL and DNB column (250 × 4.6 mm) at 35 °C with detection at 237 nm. The eluant was 90% hexane/10% isopropyl alcohol with 0.1% trifluoroacetic acid, pumped at 1.5 ml/min. Retention times of the (*S*)-(-)- and (*R*)-(+)-MTSO enantiomers were 23.2 and 25.2 min, respectively. Separate standard curves were run with chiral separation for each enantiomer with a linear range of standard (2.5 to 20 nmol). The detection limits for (*R*)-(+)-MTSO ($r^2 = 0.9975$) and (*S*)-(-)- MTSO ($r^2 = 0.9990$) were 0.2 and 0.1 nmol, respectively.

Following characterization of individual expressed FMOs, the FMO activity of female mouse lung and liver microsomes was assessed under limited conditions. Activity toward MMI was performed without pre-treating microsomes and following 10 min heat treatment at 50 °C, during which the protein concentration was 3 mg/ml in storage buffer, as already described. Assays were performed in duplicate for each microsomal pool at pH 8.5 with 2 mM MMI and 200 µg protein.

3. Results

3.1 Message levels

We wanted to select a housekeeping gene for normalization that was expressed at relatively constant levels from strain-to-strain and from liver to lung. We selected *Hprt1*, *Rpl13a*, and *Tbp* as candidates because these genes appeared to be expressed at relatively constant levels in liver and lung from humans [31]. *Actb* was included as it is commonly used for normalization. Expression levels were determined for all of the mouse samples. All of the housekeeping genes were expressed at higher mean levels in lung tissue than in liver (Fig. 1), although differences were not always significant. There were no statistical differences between strains with any of the four housekeeping genes. The largest mean fold difference (5.0-fold) in liver vs. lung expression was observed with *Rpl13a*, followed by *Actb* (3.8-fold), *Tbp* (2.8) and *Hprt1* (2.2-fold). We utilized *Hprt1* for normalization since the magnitude of expressed differences

between liver and lung tissue was less for this gene. *Hprt1* showed the least amount of variability among individual mice in both lung and liver, and on average the level of expression was closer to the message level of *Fmo* than either *Actb* or *Tbp*.

Expression levels of *Fmo1*, *Fmo2*, *Fmo3*, and *Fmo5* mRNA were quantified in lung and liver from eight strains of mice. Levels of *FMO* expressed in each mouse were normalized by the amount of *Hprt1* in the same mouse RNA sample (Fig. 2). In the lung (Fig. 2a), there were no significant differences in transcript levels among strains for *Fmo1*, *Fmo3* or *Fmo5*. The mean *Fmo2* lung transcript level among 129 mice was significantly higher than that observed among C57 ($p < 0.01$), DBA ($p < 0.01$) and SWR ($p < 0.05$) mice. In the liver (Fig. 2b) no significant differences in transcript levels among strains were detected for *Fmo1* and *Fmo3*. *Fmo2* transcript levels, while low in liver, were significantly higher in DBA mice than in A/J ($p < 0.05$) mice. *Fmo5* was significantly higher in livers of 129 mice than in either C57 ($p < 0.05$) or DBA ($P < 0.01$) mice, while levels detected in SWR mice were only higher than those observed in DBA ($p < 0.05$) mice. Variance was greatest among 129 mice for lung *Fmo2* and liver *Fmo5* owing to a single mouse that had much lower levels of both of these isoforms than the remaining three mice; however, this variability was not observed for the other *FMO* isoforms. It is possible that the strain-specific statistical differences we detected are an artifact of our limited sample size. *Fmo2* was the most abundant form expressed in lungs from all strains averaging 59% of total *FMO* message. Total *FMO* transcript abundance among the four isoforms in lung tissue showed *Fmo2* (59%) > *Fmo1* (34%) > *Fmo5* (5%) > *Fmo3* (2%) in the eight strains. Individual results from the eight strains from lung tissue were pooled and averages from each isoform were compared to *Fmo2*. The expression of *Fmo1*, *Fmo3*, and *Fmo5* was 58, 4, and 8% of *Fmo2* expression in lungs, respectively. *Fmo5* was more abundant in liver tissue from all strains than the other three *Fmo* isoforms. Transcript abundance in liver tissues showed *Fmo5* (76%) > *Fmo3* (7%) > *Fmo1* (16%) > *Fmo2* (1%). When expressed as percentages of *Fmo5*, *Fmo1*, *Fmo2*, and *Fmo3* were 21, 1, and 9% respectively of this most abundant form in liver.

3.2 Enzyme activity

The activity of expressed *Fmo1*, *Fmo2* and *Fmo3* was assessed from pH 7.5 to 9.5 using both MMI and MTS as substrate, which are exclusively and primarily metabolized by *FMOs*, respectively. *Fmo1*, *Fmo2* and *Fmo3* displayed activity throughout the entire pH range when MMI was the substrate (Fig. 3a), but each isoform had a unique pattern of pH-dependent activity. *Fmo1* and *Fmo3* achieved higher velocities than *Fmo2* at all pHs tested, except pH 9.5. *Fmo2* was the only isoform that may not have achieved maximal velocity with the pH range that was tested. A different isoform-specific, pH-dependent pattern of activity was observed when MTS was the substrate (Fig. 3b). The observed velocity increased with pH for *Fmo1* and *Fmo2*, and both of these isoforms produced only R-(+)-MTSO. Higher velocities were observed with *Fmo1* than *Fmo2* throughout the pH range, but the difference was the least at pH 9.5. *Fmo3* achieved only low velocities when MTS was the substrate, produced mixtures of the R-(+)- and S-(-)-MTSO metabolite and generated no more than a trace amount of metabolites at pH 9.5.

We selected pH 8.5 for further studies with MMI as we observed more reliability in the *Fmo1* spectrophotometric output (the oxidation rate detected displayed little deviation during the observed time interval) at this pH (data not shown), and pH 9.5 for additional studies with MTS because *Fmo2* was our primary isoform of interest and we could eliminate virtually all *Fmo3* contributions under these conditions. Addition of 1% sodium cholate to the reaction mixture for MMI metabolism marginally increased the activity of *Fmo2* to 107% of untreated, but decreased the activity of *Fmo1* and *Fmo3* to 52 and 68%, respectively (Fig. 3c). Increasing the detergent concentration to 1.5% decreased the activity of all of the isoforms. *Fmo2* retained

86% of its activity under these conditions, while Fmo1 and Fmo3 retained 15 and 39% activity respectively. Heat-treating the microsomal samples prior to assay was a more effective means of eliminating Fmo1 and Fmo3 activity while retaining most of the Fmo2 activity (Fig. 3c). The activity retained after heating with either MMI or MTS as the substrate was very similar, 94 to 96% for Fmo2, and 2-3% retention for Fmo1.

Calculated kinetic parameters demonstrate that Fmo1 is more efficient at MTS oxidation than Fmo2 (Table 4) under our standard assay conditions. MTS was a good substrate for both isoforms but the K_m for Fmo2, 10.2 μM , was more than three times higher than that observed for Fmo1, 3.2 μM . Coupling the low K_m of Fmo1 with the higher k_{cat} for this enzyme yielded a mean specificity constant estimate of 56.1 $\text{min}^{-1} \mu\text{M}^{-1}$, compared with the significantly lower ($P < 0.05$) but very respectable specificity constant of 7.5 $\text{min}^{-1} \mu\text{M}^{-1}$ for Fmo2. To our knowledge the specificity constant that we have estimated for MTS oxidation by Fmo1 is about six-fold higher than what has been published for any FMO with any substrate, and in our own laboratory have only estimated a higher specificity constant for the oxidation of tetrahydrothiophene oxidation by human FMO2.1 (unpublished results).

We used our un-normalized measurement of FMO transcript levels together with our estimates of activity (unheated vs. heated), with MMI as substrate, to predict the level of retained activity that we should observe with heated lung and liver microsomes (Table 5). We predicted that we would observe 35.6% retained activity with lung microsomes and 4.2% activity with liver microsomes. Unheated activity for lung and liver was 21.2 (S.D. 7.1) and 22.0 (S.D. 1.6) nmol TNB oxidized $\text{min}^{-1} \text{mg}^{-1}$ protein, respectively. We observed 41.4% (S.D. 6.4%) retained activity with lung microsomes and 5.8% (S.D. 2.8%) retained activity with liver microsomes.

4. Discussion

This paper explores the co-expression of *Fmo* genes in mouse lung and liver and provides an initial systematic characterization of enzymatic properties of Fmo1, Fmo2 and Fmo3. Fmo5 was included for transcriptional studies for methods verification, but was not included for enzymatic studies since it has not so far been demonstrated to metabolize any drugs or xenobiotics to a significant degree. The goal of this work was to determine if a single mouse *Fmo2* knockout would model human *Fmo2* expression, or if a double knockout would be required. Enzyme characterization was undertaken to determine the best conditions for studying contributions from individual FMOs in the event that multiple isoforms were co-expressed in target organs.

If correct, recent findings [26] indicating that *Fmo2* transcript was nearly absent from the lungs of 129 and C57 mice, from 0 to 8 weeks of age, would render meaningless any efforts to develop an *Fmo2* knockout mouse. We hypothesized that strain differences might exist that would account for the lack of *Fmo2* transcript they measured and would explain the presence of both *Fmo2* transcript and Fmo2 enzyme activity from the lungs of ICR (CD-1) mice [25]. We included mice from these three strains in our study and added five additional strains. We worked with eight-week old mice and used the same forward and reverse primer sequences for *Fmo1*, *Fmo3* and *Fmo5* as were used to isolate cDNA clones for RNase protection studies [26]. When we initiated the study, we designed a different set of primers for *Fmo2*, as the published forward primer sequence did not match (28.5% overall mismatch; 11.1% 3' end mismatch) NCBI's *Fmo2* cDNA reference sequence ([NM_018881](#)). Interestingly, new real-time PCR studies performed by the Shephard and Phillips laboratory, in response to our findings, with *Fmo2* primers designed to a different upstream region of the gene, and RNA isolated from a new set of male C57 mice reconfirmed the pattern of *Fmo1-4* transcript abundance that they originally reported (personal communication, E. Shephard). Thus the source of inter-laboratory differences in relative *Fmo2* transcript levels is, at present, unknown.

Our findings verify that there is significant production of *Fmo1* transcript in mouse lung, which is in keeping with both earlier studies [25,26]. However, in contrast to the 2004 study [26], we found *Fmo2* transcript levels to be about 1.7-fold higher than *Fmo1* transcript levels in mouse lung. We did not detect strain differences in the pattern of *FMO* isoforms expressed. Absolute transcript levels that we measured were consistently lower (except for *Fmo2*) than those estimated by RNase protection [26]. However when we expressed *FMO* levels in female mice as ratios the methods provided quite consistent results. We estimated that the ratio of *Fmo1:Fmo5* was 7.0 in lung and 0.2 in liver, compared with 4.5 and 0.2, respectively, by RNase protection. We estimated that the ratio of *Fmo1:Fmo3* was 15.2 in lung and 2.2 in liver, compared with approximately 14.0 and 0.5, respectively, by RNase protection. Thus our data for *Fmo1*, *Fmo3* and *Fmo5* is consistent with published work, except that our mice, for unknown reasons, had relatively less *Fmo3* in liver.

MTS sulfoxidation has been used to simultaneously discriminate *FMO1*, *FMO3* and *FMO5* from rabbit [32] based on kinetic parameters and prochiral selectivity. MTS was primarily metabolized by *FMOs*, although cytochrome P450 can contribute to the sulfoxidation of MTS. MTS was not a significant substrate for rabbit *FMO5*, but was a substrate for *FMO1*, *FMO2* and *FMO3*. *FMO1* and *FMO2* both had an apparent $K_m < 10 \mu\text{M}$, while *FMO3* had a low affinity K_m of $270 \mu\text{M}$. *FMO3* was additionally distinguishable from *FMO1* and *FMO2* because it produced a mixture of the (R)- and (S)-sulfoxide, while *FMO1* and *FMO2* essentially produced only the (R)-sulfoxide product but could be distinguished because they are not co-expressed in rabbit tissues.

Commercially available human *FMO5* generated insignificant levels of MTS sulfoxidation and no oxidative activity at all toward the environmentally important *FMO* substrates alpha-naphthylthiourea and phorate (data not shown). Thus, while we found abundant *Fmo5* transcript in liver, in agreement with earlier work [26], we postulate a negligible enzymatic contribution from this isoform.

Our results for MTS metabolism with mouse *Fmo1*, *Fmo2* and *Fmo3* follow the same pattern reported for rabbit isoforms [32]. *Fmo3* produced only low levels of sulfoxide, but depending on pH, produced varying proportions of the (R)- and (S)-sulfoxides. By restricting analysis to pH 9.5 we could virtually eliminate any contribution of *Fmo3* to activity. This strategy should be particularly useful for the study of *Fmo1* in mouse liver that expresses almost no *Fmo2*. Because both *Fmo1* and *Fmo2* had high affinity for MTS and produced only detectable (R)-sulfoxide, we will have to couple this assay with an additional parameter to separate contributions by *Fmo1* and *Fmo2* in tissues such as lung that co-express these *FMOs*. In our study, heating the expressed baculosome samples for 10 min at 50°C virtually eliminated the *Fmo1* contribution (and *Fmo3* as well); thus in lung microsomes 96% of the measured activity after heat treatment was predicted to be due to *Fmo2*.

By combining our estimates of transcript level with data from characterization of expressed isoform activity, we were able to predict the relative activity we should observe in unheated and heated microsomes prepared from mouse lung and liver tissue. The high degree of concordance in predicted and observed activity from lung and liver microsomes is independent confirmation of *FMO* transcript levels we measured in these tissues. By carefully controlling protein concentration and buffer conditions during microsomal pre-heating, previously demonstrated to be critical for generating reproducible data [16,33], we have identified conditions where at least 95% of the activity in mouse lung microsomes should be due to *Fmo2*. This multiple assay procedure to assess *Fmo2* contributions will be necessary until an *Fmo2*-specific substrate can be identified.

In studies designed to determine which member of a gene family, e.g. CYPs, are responsible for metabolism of a given xenobiotic, antibody inhibition has proven to be a valuable approach. The relative contribution of a specific CYP can be determined by adding increasing amounts of polyclonal antibody, specific for that CYP, to the reaction mixture. If that CYP is the major or sole form active toward that substrate, 90% or more of the activity can be eliminated. Unfortunately, without exception, polyclonal antibodies raised to FMOs have weak or no effect on catalytic activity. Additionally, most antibodies to FMO have at least some cross-reactivity to multiple isoforms.

Another tool used in such studies are enzyme-specific inhibitors, including mechanism-based (or suicide substrate) inhibitors. Most CYPs have at least one inhibitor identified with high specificity. However, other than competitive substrates, there are no inhibitors of FMO and certainly no isoform-specific inhibitors. The use of substrate specificity has provided only limited value in identification of the activity of a particular FMO.

We have not attempted to directly compare the total content of FMO in lung and liver. Because housekeeping gene levels were not equivalent in these tissues, normalized data could not be used for this purpose. Although transcript levels of *Fmo1*, *Fmo2* and *Fmo3* were higher in lung tissue, the RNA content per cell is higher in mouse liver than lung [34]. Nonetheless, as unheated activity toward MMI was virtually identical in unheated lung and liver microsomes and *Fmo1* has much higher activity toward MMI than does *Fmo2*, the combined *Fmo1-3* content of lung microsomes must have been higher than in liver microsomes.

Our evidence that *Fmo2* transcript is the major lung *Fmo* isoform and evidence that activity in lung microsomes verifies results of mouse [25] and rat [24] studies that identify both *Fmo1* and *Fmo2* in the lung of these species by transcript detection and enzyme activity. We found that our predictions of the relative amount of activity that would be retained in heated lung and liver microsomes, based on determinations of *FMO* transcript levels and activity retention by individual isoforms, closely mirrored the observed activity in liver and lung microsomes. The somewhat higher level of observed retained activity than we had predicted indicates a possibility that we may have underestimated *Fmo2* transcript levels, that there has been some compromise of *Fmo1* activity in the tissues we purchased, or that transcript abundance and enzyme assays need to be determined from the same animals for absolute concordance of methods.

Because *Fmo1* message levels were significant in the lung of all mouse strains evaluated, and given that substrates of *Fmo2* are usually substrates of *Fmo1*, it will be necessary to develop an *Fmo1/Fmo2* double knockout to confidently model the phenotypes associated with the human *FMO2* genetic polymorphism. An *Fmo1* knockout mouse will model the Hispanic and African American individuals that express active *FMO2*, while the *Fmo1/Fmo2* double knockout will model the majority of the human population that does not express active *FMO2* protein. Given that all mouse strains tested had similar *FMO* profiles, any genetic background should work in future studies.

Acknowledgements

Part of this work was presented at the Fourteenth North American meeting of the International Society for the Study of Xenobiotics (October 22-26, 2006, Rio Grande, Puerto Rico). This study was supported by PHS Grant HL038650. We also acknowledge support from the Cell Culture Facility Core of the Oregon State University Environmental Health Sciences Center (ES 00210).

References

1. Krueger SK, Williams DE. Mammalian flavin-containing monooxygenases: structure/function, genetic polymorphisms and role in drug metabolism. *Pharmacol Ther* 2005;106:357–87. [PubMed: 15922018]

2. Guo WX, Poulsen LL, Ziegler DM. Use of thiocarbamides as selective substrate probes for isoforms of flavin-containing monooxygenases. *Biochem Pharmacol* 1992;44:2029–37. [PubMed: 1449520]
3. Kim YM, Ziegler DM. Size limits of thiocarbamides accepted as substrates by human flavin-containing monooxygenase 1. *Drug Metab Dispos* 2000;28:1003–6. [PubMed: 10901713]
4. Smith PB, Crespi C. Thiourea toxicity in mouse C3H/10T12 cells expressing human flavin-dependent monooxygenase 3. *Biochem Pharmacol* 2002;63:1941–8. [PubMed: 12093470]
5. Henderson MC, Krueger SK, Stevens JF, Williams DE. Human flavin-containing monooxygenase form 2 S-oxygenation: sulfenic acid formation from thioureas and oxidation of glutathione. *Chem Res Toxicol* 2004;17:633–40. [PubMed: 15144220]
6. Lawton MP, Cashman JR, Cresteil T, Dolphin CT, Elfarra AA, Hines RN, et al. A nomenclature for the mammalian flavin-containing monooxygenase gene family based on amino acid sequence identities. *Arch Biochem Biophys* 1994;308:254–7. [PubMed: 8311461]
7. Hernandez D, Janmohamed A, Chandan P, Phillips IR, Shephard EA. Organization and evolution of the flavin-containing monooxygenase genes of human and mouse: identification of novel gene and pseudogene clusters. *Pharmacogenetics* 2004;14:117–30. [PubMed: 15077013]
8. Hines RN, Hopp KA, Franco J, Saeian K, Begun FP. Alternative processing of the human FMO6 gene renders transcripts incapable of encoding a functional flavin-containing monooxygenase. *Mol Pharmacol* 2002;62:320–5. [PubMed: 12130684]
9. Williams DE, Ziegler DM, Nordin DJ, Hale SE, Masters BS. Rabbit lung flavin-containing monooxygenase is immunochemically and catalytically distinct from the liver enzyme. *Biochem Biophys Res Commun* 1984;125:116–22. [PubMed: 6439199]
10. Tynes RE, Sabourin PJ, Hodgson E. Identification of distinct hepatic and pulmonary forms of microsomal flavin-containing monooxygenase in the mouse and rabbit. *Biochem Biophys Res Commun* 1985;126:1069–75. [PubMed: 3919719]
11. Lawton MP, Gasser R, Tynes RE, Hodgson E, Philpot RM. The flavin-containing monooxygenase enzymes expressed in rabbit liver and lung are products of related but distinctly different genes. *J Biol Chem* 1990;265:5855–61. [PubMed: 2318837]
12. Nikbakht KN, Lawton MP, Philpot RM. Guinea pig or rabbit lung flavin-containing monooxygenases with distinct mobilities in SDS-PAGE are allelic variants that differ at only two positions. *Pharmacogenetics* 1992;2:207–16. [PubMed: 1306120]
13. Yueh M-F, Krueger SK, Williams DE. Pulmonary flavin-containing monooxygenase (FMO) in rhesus macaque: expression of FMO2 protein, mRNA and analysis of the cDNA. *Biochim Biophys Acta* 1997;1350:267–71. [PubMed: 9061021]
14. Zhang J, Cashman JR. Quantitative analysis of FMO gene mRNA levels in human tissues. *Drug Metab Dispos* 2006;34:19–26. [PubMed: 16183778]
15. Dolphin CT, Beckett DJ, Janmohamed A, Cullingford TE, Smith RL, Shephard EA, et al. The flavin-containing monooxygenase 2 gene (FMO2) of humans, but not of other primates, encodes a truncated, nonfunctional protein. *J Biol Chem* 1998;273:30599–607. [PubMed: 9804831]
16. Krueger SK, Martin SR, Yueh MF, Pereira CB, Williams DE. Identification of active flavin-containing monooxygenase isoform 2 in human lung and characterization of expressed protein. *Drug Metab Dispos* 2002;30:34–41. [PubMed: 11744609]
17. Whetstine JR, Yueh M-F, McCarver DG, Williams DE, Park C-S, Kang JH, et al. Ethnic differences in human flavin-containing monooxygenase 2 (FMO2) polymorphisms: detection of expressed protein in African-Americans. *Toxicol Appl Pharmacol* 2000;168:216–24. [PubMed: 11042094]
18. Furnes B, Feng J, Sommer SS, Schlenk D. Identification of novel variants of the flavin-containing monooxygenase gene family in African Americans. *Drug Metab Dispos* 2003;31:187–93. [PubMed: 12527699]
19. Krueger SK, Williams DE, Yueh MF, Martin SR, Hines RN, Raucy JL, et al. Genetic polymorphisms of flavin-containing monooxygenase (FMO). *Drug Metab Rev* 2002;34:523–32. [PubMed: 12214664]
20. Krueger SK, Siddens LK, Martin SR, Yu Z, Pereira CB, Cabacungan ET, et al. Differences in Fmo2*1 allelic frequency between hispanics of Puerto Rican and Mexican descent. *Drug Metab Dispos* 2004;32:1337–40. [PubMed: 15355885]

21. Krueger SK, Siddens LK, Henderson MC, Andreasen EA, Tanguay RL, Pereira CB, et al. Haplotype and functional analysis of four flavin-containing monooxygenase isoform 2 (FMO2) polymorphisms in Hispanics. *Pharmacogenet Genomics* 2005;15:245–56. [PubMed: 15864117]
22. Henderson MC, Krueger SK, Siddens LK, Stevens JF, Williams DE. S-oxygenation of the thioether organophosphate insecticides phorate and disulfoton by human lung flavin-containing monooxygenase 2. *Biochem Pharmacol* 2004;68:959–67. [PubMed: 15294458]
23. Lattard V, Longin-Sauvageon C, Krueger SK, Williams DE, Benoit E. The FMO2 gene of laboratory rats, as in most humans, encodes a truncated protein. *Biochem Biophys Res Commun* 2002;292:558–63. [PubMed: 11906197]
24. Hugonnard M, Benoit E, Longin-Sauvageon C, Lattard V. Identification and characterization of the FMO2 gene in *Rattus norvegicus*: a good model to study metabolic and toxicological consequences of the FMO2 polymorphism. *Pharmacogenetics* 2004;14:647–55. [PubMed: 15454729]
25. Venkatesh K, Blake B, Levi PE, Hodgson E. The flavin-containing monooxygenase in mouse lung: evidence for expression of multiple forms. *J Biochem Toxicol* 1992;7:163–9. [PubMed: 1479594]
26. Janmohamed A, Hernandez D, Phillips IR, Shephard EA. Cell-, tissue-, sex- and developmental stage-specific expression of mouse flavin-containing monooxygenases (Fmos). *Biochem Pharmacol* 2004;68:73–83. [PubMed: 15183119]
27. Guengerich, FP. Analysis and characterization of enzymes. In: Hayes, AW., editor. *Principles and Methods of Toxicology*. Raven Press; New York: 1989. p. 777-814.
28. Bradford MM. A rapid and sensitive method for the quantitation of microgram quantities of protein utilizing the principle of protein-dye binding. *Anal Biochem* 1976;72:248–54. [PubMed: 942051]
29. Dixit A, Roche TE. Spectrophotometric assay of the flavin-containing monooxygenase and changes in its activity in female mouse liver with nutritional and diurnal conditions. *Arch Biochem Biophys* 1984;233:50–63. [PubMed: 6087744]
30. Rettie AE, Bogucki BD, Lim I, Meier GP. Stereoselective sulfoxidation of a series of alkyl p-tolyl sulfides by microsomal and purified flavin-containing monooxygenases. *Mol Pharmacol* 1990;37:643–51. [PubMed: 2338943]
31. Vandesompele J, De Preter K, Pattyn F, Poppe B, Van Roy N, De Paepe A, et al. Accurate normalization of real-time quantitative RT-PCR data by geometric averaging of multiple internal control genes. *Genome Biol* 2002;3(RESEARCH0034):1–12.
32. Rettie AE, Lawton MP, Sadeque AJ, Meier GP, Philpot RM. Prochiral sulfoxidation as a probe for multiple forms of the microsomal flavin-containing monooxygenase: studies with rabbit FMO1, FMO2, FMO3, and FMO5 expressed in *Escherichia coli*. *Arch Biochem Biophys* 1994;311:369–77. [PubMed: 8203899]
33. Krueger SK, Yueh M-F, Martin SR, Pereira CB, Williams DE. Characterization of expressed full-length and truncated FMO2 from rhesus monkey. *Drug Metab Dispos* 2001;29:693–700. [PubMed: 11302936]
34. Kanno J, Aisaki K, Igarashi K, Nakatsu N, Ono A, Kodama Y, et al. “Per cell” normalization method for mRNA measurement by quantitative PCR and microarrays. *BMC Genomics* 2006;7:64. [PubMed: 16571132]

Abbreviations

Actb	β -actin
Hprt1	hypoxanthine guanine phosphoribosyl transferase 1
FMO	flavin-containing monooxygenase
MMI	methimazole

MTS	methyl <i>p</i> -tolyl sulfide
MTSO	methyl <i>p</i> -tolyl sulfoxide
Rpl13a	large ribosomal protein 13a
Tbp	TATA box binding protein

and the following mouse strains:

A/J	A/J
C57BL/6J	C57
DBA/2J	DBA
FVB/NJ	FVB
SWR/J	SWR
129S1/SvImJ	129
Hsd:ICR (CD-1)	ICR
B6129SF1/J	F1 Hyb

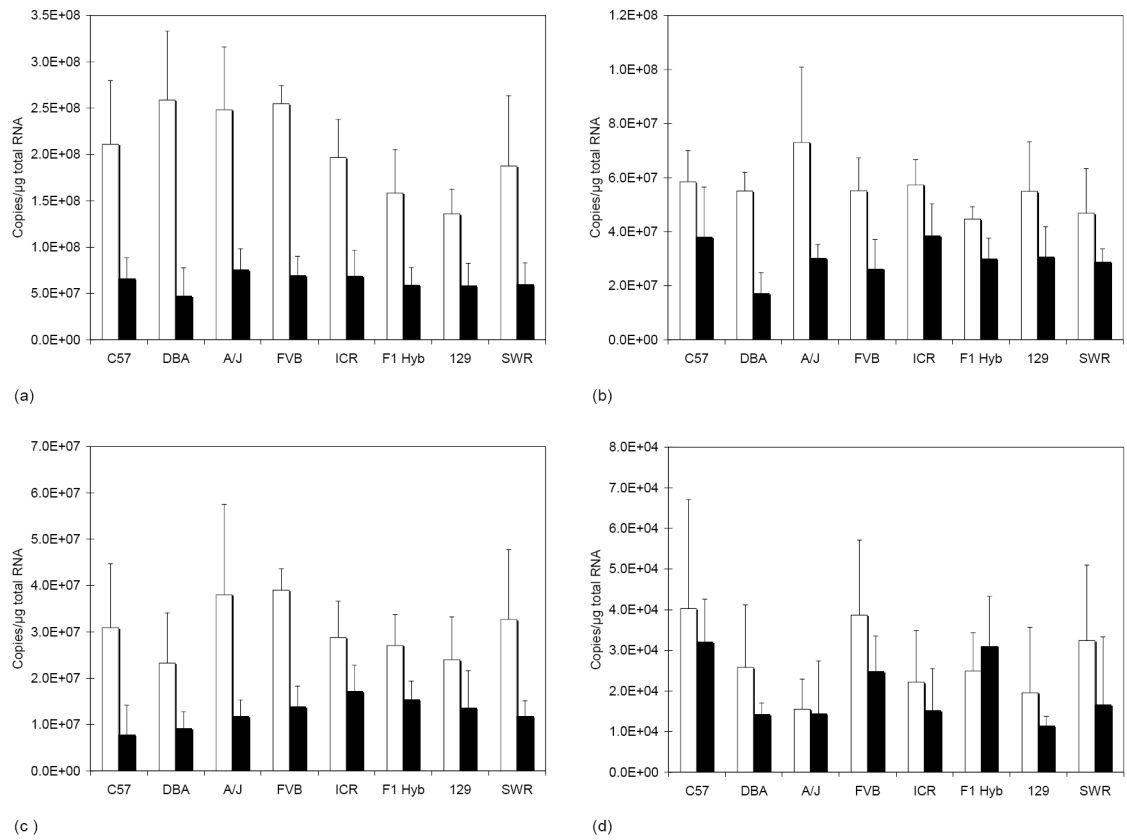


Fig.1. Message level of housekeeping genes in mouse lung and liver. The mean \pm S.D. strain ($n =$ four per strain) message level in lung (white bars) and liver (black bars) is plotted for *Actb* (A), *Hprt1* (B), *Rpl13a* (C) and *Tbp* (D).

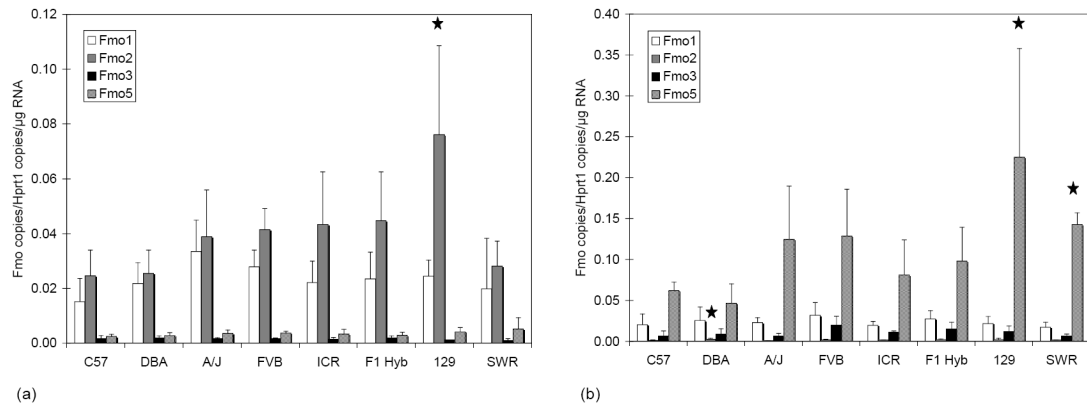
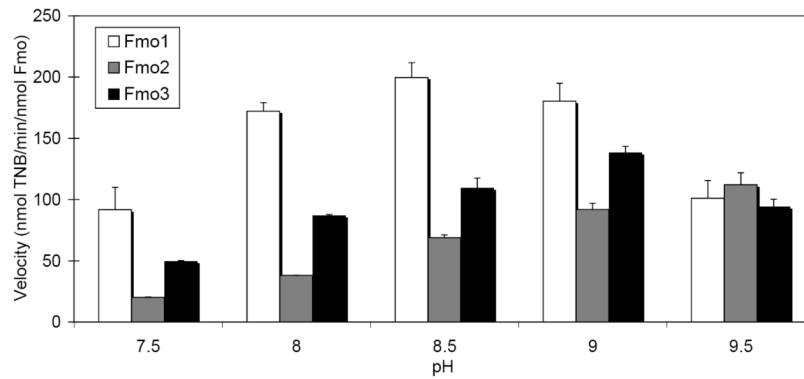
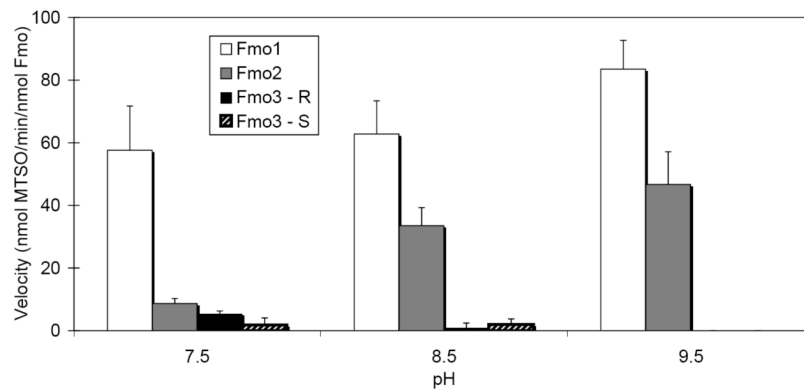


Fig. 2.

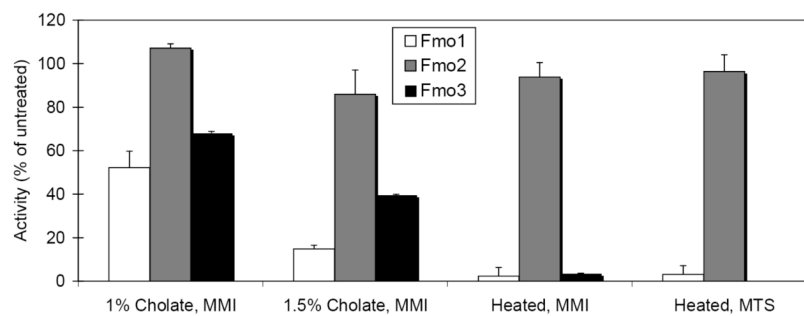
FMO message levels in mouse lung and liver. Graphs show mean \pm S.D. strain (n = four per strain) message levels of *Fmo1*, *Fmo2*, *Fmo3* and *Fmo5* plotted for lung (A), and liver (B). Stars indicate transcript levels for the indicated strain were significantly different than other strains as follows: (A) lung *Fmo2* transcript levels for 129 were higher than those observed for C57 and DBA ($p < 0.01$), as well as SWR ($p < 0.05$); (B) liver *Fmo2* transcript levels for DBA were higher than levels for A/J ($p < 0.05$); (B) liver *Fmo5* transcript levels for 129 were higher than levels in C57 ($p < 0.05$) and DBA ($p < 0.01$), while levels in SWR were higher than in DBA ($p < 0.05$).



(a)



(b)



(c)

Fig. 3. Enzyme activity of mouse Fmo1, Fmo2 and Fmo3. Mean FMO activity is shown as a function of pH with 2 mM MMI (A), or 200 μ M MTS (B) as substrate. Mean residual FMO activity is shown on addition of sodium cholate (pH 8.5 with 2 mM MMI) or after heating for 10 min at 50 $^{\circ}$ C (pH 8.5 with 2 mM MMI, or pH 9.5 with 200 μ M MTS) (C). Error bars indicate S.D. (n = two to six assays per condition).

Table 1

Mouse strains and sources.

Mouse Strain	Abbreviation	Strain Type	Source
A/J	A/J	Inbred	Jackson Lab
C57BL/6J	C57	Inbred	Jackson Lab
DBA/2J	DBA	Inbred	Jackson Lab
FVB/NJ	FVB	Inbred	Jackson Lab
SWR/J	SWR	Inbred	Jackson Lab
129S1/SvImJ	129	Inbred	Jackson Lab
Hsd:ICR (CD-1)	ICR	Outbred	Harlan Lab
B6129SF1/J ^a	F1 Hyb	F1 Hybrid	Jackson Lab

^aC57BL6J female × 129S1/SvImJ male.

Table 2

Primers used for quantitative PCR of mouse FMO and housekeeping genes.

Gene	Primer Sequence (5' to 3')	Exon	Amplicon Size (bp)	Annealing Temperature	ENSEMBLE Transcript ¹	Reference
<i>Fmo1</i>	5'-TGTCCTGGACAGTGGGAAGT	4	217	56	ENSMUST00000046049	[26]
	5'-CATTCCAACTACAAGGACTCG	5				
<i>Fmo2</i>	5'-AGGCTCCATCTCCCAACCGTA	7	382	56	ENSMUST00000045902	
	5'-CCGGTCTTTAAGGGTTTCAGG	9				
<i>Fmo3</i>	5'-CACCACTGAAAAGCACGGTA	4	445	58	ENSMUST00000028010	[26]
	5'-GTTTTAAAGGCACCAAAACCATAG	6				
<i>Fmo5</i>	5'-ATCACACGGATGCTCACCTG	4	235	58	ENSMUST00000029729	[26]
	5'-GCTTGGCTACACGGTTCAAG	6				
<i>Hprt1</i>	5'-AGCTACTGTAATGATCAGTCAAC	3/4	180	53	ENSMUST00000026723	RT Primer DB ID:50 ²
	5'-AGAGGTCTCTTTCACACGCA	7				
<i>Rpl13a</i>	5'-GCTCTCAAAGGTGTTCGGCTGA	6	157	53	ENSMUST00000102669	
	5'-AGATCTGCTTCTTCTCCGATA	7				
<i>Thp</i>	5'-GGCCTCTCAGAAGCATCACT	2/3	167	53	ENSMUST00000039079	RT Primer DB ID:49 ²
	5'-GCCAAGCCCTGAGCATAA	3				
<i>Actb</i>	5'-CTACAGCTTACCACCACACAG	4	137	62	ENSMUST00000031564	
	5'-GCAGCTCATAGCTTCTTCC	4				

¹ <http://www.ensembl.org/index.html>

² <http://medgen.ugent.be/r/primerdb/>

Table 3Primers used to clone mouse *Fmo1*, *Fmo2* and *Fmo3*.

Isoform	Primer Type	Primer Sequence 5' to 3' ^a
<i>Fmo1</i>	Forward	5'-CACC <u>ATG</u> GCA AAG CGA GTG GCA AT
<i>Fmo1</i>	Reverse	5'- <u>TTA</u> CAG GAA AAT CAA GAA GAC AGC T
<i>Fmo2</i>	Forward	5'-CACC <u>ATG</u> GCA AAG AAG GTT G
<i>Fmo2</i>	Reverse	5'- <u>TTA</u> AAA CCC CTG AAG TTG GA
<i>Fmo3</i>	Forward	5'-CACC <u>ATG</u> AAG AAG AAA GTG GCC ATC
<i>Fmo3</i>	Reverse	5'- <u>TCA</u> GAT CAA CAC AAG GAA CAA AGC

^a Italicized nucleotides were added for vector compatibility. The sequences corresponding to start and stop codons are underlined.

Table 4
Kinetic constants for MTS metabolism at pH 9.5 by Fmo1 and Fmo2.

Isoform	K_m^a	k_{cat}^b	k_{cat}/K_m
Fmo1	3.6 (2.3) ^c	176 (57)	56.1 (19.7)
Fmo2	10.2 (2.5)	75 (22)	7.5 (0.4)

^aThe K_m is in micromolar units.

^bThe reported k_{cat} was calculated as nmoles MTSO formed $\text{min}^{-1} \text{nmol}^{-1}$ FMO.

^cMean and (S.D.) from analysis of two independently expressed batches of protein.

Predicted pre- and post-heat activity for the major drug-metabolizing FMOs in an average mouse lung and liver.

Table 5

Parameter	Units	Isoform contribution			Total activity
		Fmo1	Fmo2	Fmo3	
Unheated activity ^a	nmol/min/nmol Fmo	199.8	68.9	109.5	
Heated activity ^b	nmol/min/nmol Fmo	4.6	64.6	3.6	
Observed transcript copy number ^c		1.4×10^6	Lung 2.4×10^6	9.2×10^4	
Relative abundance of <i>Fmo</i> ^d		0.58	1.0	0.04	
Contribution to unheated activity ^e	nmol/min/nmol Fmo	115.9	68.9	4.4	189.2
Contribution to heated activity ^f	Percent of total	61.3	36.4	2.3	100.0
	nmol/min/nmol Fmo	2.7	64.6	0.1	67.4
	Percent of total	4.0	95.8	0.1	99.9
	Percent retained activity				35.6
Observed transcript copy number ^c		7.1×10^5	Liver 4.8×10^4	3.3×10^5	
Relative abundance of <i>Fmo</i> ^d		1.0	0.07	0.47	
Contribution to unheated activity ^e	nmol/min/nmol Fmo	199.8	4.8	51.5	256.1
Contribution to heated activity ^f	Percent of total	78.0	1.9	20.1	100.0
	nmol/min/nmol Fmo	4.6	4.5	1.7	10.8
	Percent of total	42.6	41.7	15.7	100.0
	Percent retained activity				4.2

^aMean velocity at pH 8.5 for metabolism of MMI by a single isoform; from Fig. 3a.

^bMean velocity after heating; metabolism of MMI by a single isoform at pH 8.5.

^cMean un-normalized *FMO* transcript copy number/ μ g RNA from eight mouse strains (n = 32).

^dProportion of total transcript copy number of *Fmo1* + *Fmo2* + *Fmo3*.

^eRelative abundance \times unheated activity.

^fRelative abundance \times heated activity.